Inorganica Chimica Acta 397 (2013) 88–93

Contents lists available at SciVerse ScienceDirect

Inorganica Chimica Acta

journal homepage: www.elsevier.com/locate/ica

Two different dimensional bbbm-based cobalt(II) coordination polymers tuned by benzenedicarboxylates: Assembly, structures and properties

Xiu-Li Wang *, Li-Li Hou, Ju-Wen Zhang *, Guo-Cheng Liu, Bao Mu, Hong-Yan Lin

Department of Chemistry, Bohai University, Liaoning Province Silicon Materials Engineering Technology Research Center, Jinzhou 121000, PR China

ARTICLE INFO

Article history:
Received 20 July 2012
Received in revised form 5 November 2012
Accepted 16 November 2012
Available online 12 December 2012

Keywords:
Bis(benzimidazole)-based ligand
Benzenedicarboxylate
Coordination polymer
Crystal structure
Electrochemical property

ABSTRACT

Two new metal–organic coordination polymers $[Co_4(bbbm)_4(1,2\text{-}BDC)_4(H_2O)]\cdot 2H_2O$ (**1**) and [Co(bbbm)(1,4-BDC)] (**2**) (bbbm = 1,1-(1,4-butanediyl)bis-1H-benzimidazole, 1,2-H_2BDC = 1,2-benzenedicarboxylic acid and 1,4-H_2BDC = 1,4-benzenedicarboxylic acid) were obtained under hydrothermal conditions and structurally characterized. Polymer **1** exhibits a two-dimensional (2D) 4-connected network with the Co^{II} ions as four-connected nodes, and the bbbm and 1,2-BDC ligands as linkers. Polymer **2** possesses a novel three-dimensional (3D) 3-fold interpenetrated framework. The position of carboxyl groups for benzenedicarboxylates dominates the final structures of **1** and **2**. Furthermore, elemental analysis, IR spectroscopy, thermogravimetric analysis, electrochemical properties and solid state fluorescence for **1** and **2** were investigated.

1. Introduction

The construction of novel metal–organic coordination polymers (MOCPs) has received much attention due to their promising application in chemical separation [1,2], proton conductivity [3–5], selective adsorption [6,7], luminescence [8–10], magnetic materials [11–13], etc. The selection of suitable organic ligands plays crucial roles in the constructions of desirable MOCPs. In the past decade, the self-assembly of MOCPs based on the flexible bis(imidazole), bis(triazolyl) and bis(tetrazole) derivatives and polycarboxylates mixed ligands has been of an attractive area of research [14–16], which is usually based on the following reasons: (i) the flexible N-donor linkers may adopt diverse conformation when they are coordinated to the central metal ions [17]; (ii) multidentate carboxylate ligands are extensively applied in the constructions of high dimensional MOCPs due to their various coordination modes [18–20]. As is known, the constructions of MOCPs based on the flexible bis(benzimidazole) and auxiliary polycarboxylate system have been already reported [21–26]. However, the systematic studies on the effect of position of carboxyl groups for aromatic polycarboxylates on the structures of MOCPs based on the flexible bis(benzimidazole)-based ligands are still limited in the literatures.

In this work, in order to explore the effect of carboxyl position of polycarboxylate linkers on the structures of MOCPs based on the flexible 1,1-(1,4-butanediyl)bis-1H-benzimidazole (bbbm) ligand, two types of benzenedicarboxylic acids, namely, 1,2-benzenedicarboxylic acid (1,2-H_2BDC) and 1,4-benzenedicarboxylic acid (1,4-H_2BDC) were selected as auxiliary ligands to construct the target coordination polymers (Scheme 1). As a result, two coordination polymers $[Co_4(bbbm)_4(1,2\text{-}BDC)_4(H_2O)]\cdot 2H_2O$ (**1**) and [Co(bbbm)(1,4-BDC)] (**2**), were obtained and their syntheses, crystal structures, electrochemical and luminescent properties were reported.

2. Experimental

2.1. Materials and measurements

All reagents were purchased from commercial sources and used without further purification. Ligand bbbm was synthesized according to the literature method [27]. FT-IR data were collected on a Magna FT-IR 560 spectrometer (KBr pellets). Elemental analyses were performed on a Perkin-Elmer 2400 CHN elemental analyzer (C, H and N). Thermogravimetric analyses (TGA) were measured on a Pyris Diamond TG/DTA under a N_2 atmosphere with a heating rate of 10 °C min^{-1}. Fluorescence spectra were recorded on a Hitachi F-4500 fluorescence/phosphorescence spectrophotometer at room temperature. Electrochemical measurements were carried out on a CHI 440 electrochemical workstation. A conventional three-electrode system was used at room temperature. The title polymer chemically bulk-modified carbon paste electrodes (CPE) were used as the working electrodes. A saturated calomel electrode (SCE) was used as the reference electrode, and a platinum wire as the auxiliary electrode.

---

* Corresponding authors. Tel.: +86 416 3400158 (X.-L. Wang), tel.: +86 416 3400308 (J.-W. Zhang).

E-mail addresses: wangxiuli@bhu.edu.cn (X.-L. Wang), juwenzhang@yahoo.cn (J.-W. Zhang).

0020-1693/$ - see front matter © 2012 Elsevier B.V. All rights reserved.
http://dx.doi.org/10.1016/j.ica.2012.11.024

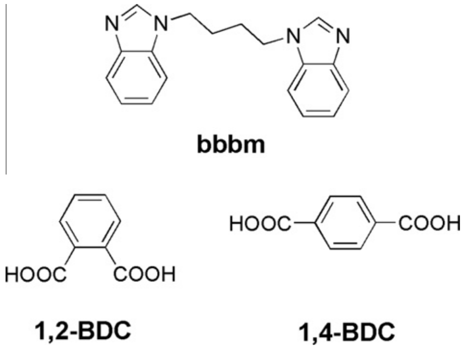

Scheme 1. The bbbm ligand and benzenedicarboxylic acids in this paper.

2.2. Syntheses of **1** and **2**

2.2.1. Synthesis of [$Co_4(bbbm)_4(1,2\text{-}BDC)_4(H_2O)]\cdot 2H_2O$ (**1**)

Polymer **1** was synthesized by hydrothermal reaction. A mixture of $CoCl_2\cdot 6H_2O$ (0.024 g, 0.10 mmol), bbbm (0.015 g, 0.05 mmol), 1,2-H_2BDC (0.008 g, 0.05 mmol), H_2O (10 mL) and NaOH (0.10 mol L^{-1}, 2 mL) was stirred for 1 h in air, and then sealed in a 25 mL Teflon-lined stainless-steel autoclave at 150 °C for 72 h. The reaction system was then slowly cooled to room temperature at a rate of 4 °C h^{-1}. Purple block crystals of **1** were collected from the final reaction system by filtration and washed with distilled water and acetone. Yield: 56% (based on Co). *Anal.* Calc. for $C_{104}H_{94}Co_4N_{16}O_{19}$ (2107.66): C, 59.26; H, 4.50; N, 10.63. Found: C, 59.43; H, 4.37; N, 10.75%. IR (KBr, cm^{-1}): 3128 w, 2364 s, 2329 m, 1612 m, 1580 s, 1539 m, 1510 m, 1394 s, 1300 w, 1257 w, 829 m, 810 w, 743 s, 671 w, 545 s.

2.2.2. Synthesis of [Co(bbbm)(1,4-BDC)] (**2**)

Synthesis of **2** is similar to that of **1** except that 1,4-H_2BDC (0.025 g, 0.15 mmol) was used instead of 1,2-H_2BDC. Purple block crystals of **2** were obtained in a 47% yield based on Co. *Anal.* Calc. for $C_{26}H_{22}CoN_4O_4$ (513.41): C, 60.82; H, 4.32; N, 10.91. Found: C, 60.98; H, 4.21; N, 11.07%. IR (KBr, cm^{-1}): 2357 s, 1619 m, 1556 m, 1494 w, 1385 s, 1170 m, 828 s, 739 s, 650 s, 596 w, 559 w.

2.3. Preparation of **1** and **2**-CPEs

Polymer **1** bulk-modified carbon paste electrode (**1**-CPE) was fabricated as follows: 0.030 g of **1** and 0.500 g of graphite powder were mixed and ground together by the agate mortar and pestle to achieve an even mixture, and then 0.15 mL of paraffin oil was added into the mixture with stirring. The resulting mixture was packed into a glass tube with 3 mm inner diameter to a length of 8 mm, and the tube surface was wiped with the weighing paper. The electrical contact was established with a copper stick [28]. The same procedure was used for the preparation of bare CPE and **2**-CPE.

Table 1
The crystal and structure refinement data for polymers **1** and **2.**

Complexes	1	2
Formula	$C_{104}H_{94}Co_4N_{16}O_{19}$	$C_{26}H_{22}CoN_4O_4$
Formula weight	2107.66	513.41
Crystal system	monoclinic	monoclinic
Space group	$P2_1/c$	$C2/c$
a (Å)	27.993(5)	16.225(5)
b (Å)	10.587(2)	18.445(5)
c (Å)	33.716(6)	16.083(5)
α (°)	90	90
β (°)	107.199(3)	108.718(5)
γ (°)	90	90
V (Å^3)	9545(3)	4559(2)
Z	4	8
D_{calc} (g cm^{-3})	1.465	1.496
μ (mm^{-1})	0.764	0.795
F(000)	4351.0	2120.0
R_1[a] ($I > 2\sigma(I)$)	0.0880	0.0774
wR_2[b] (all data)	0.2303	0.1497
GOF on F^2	0.998	1.015

[a] $R_1 = \Sigma||F_o| - |F_c||/\Sigma|F_o|$.
[b] $wR_2 = [\Sigma w(F_o^2 - F_c^2)^2/\Sigma w(F_o^2)^2]^{1/2}$.

2.4. X-ray crystallography study

X-ray diffraction data for **1** and **2** were collected on a Bruker Smart Apex CCD diffractometer with Mo Kα radiation (λ = 0.71073 Å for **1** and λ = 0.71069 Å for **2**). The structures were solved by direct methods using the program SHELXS-97, and all non-hydrogen atoms were refined anisotropically on F^2 by the full-matrix least-squares technique using the SHELXL-97 crystallographic software package [29]. The hydrogen atoms except for those of water molecules were generated geometrically and refined with isotropic thermal parameters. The crystal data and structure refinements for **1** and **2** are listed in Table 1. Selected bond distances (Å) and angles (°) for **1** and **2** are provided in Table S1. Crystallographic data for **1** and **2** have been deposited in the Cambridge Crystallographic Data Center with CCDC reference numbers 882695 and 882696 for **1** and **2**, respectively.

3. Results and discussion

3.1. Crystal structure description

3.1.1. Crystal structure of **1**

Single crystal X-ray diffraction analysis reveals that polymer **1** crystallizes in the monoclinic space group $P2_1/c$. The asymmetric

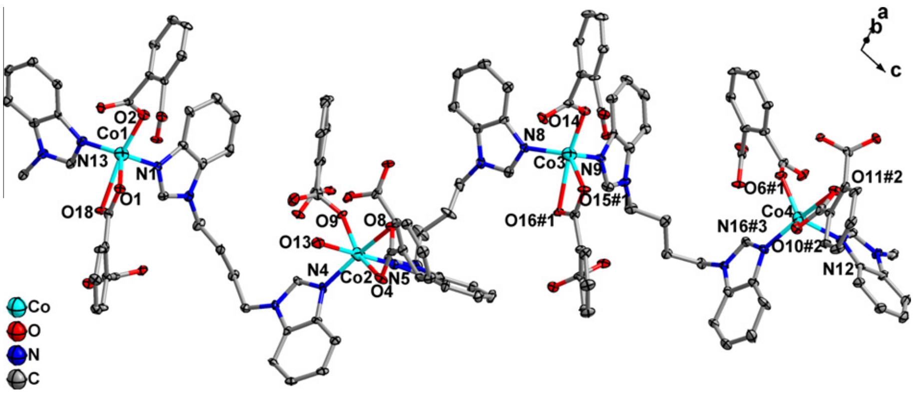

Fig. 1. Coordination environment of the Co^{II} ions in **1**. All hydrogen atoms and interstitial water molecules are omitted for clarity. Symmetry codes: #1 $-x + 1, y - 1/2, -z + 1/2$; #2 $-x + 1, y + 1/2, -z + 1/2$; #3 $x + 1, y, z + 1$.

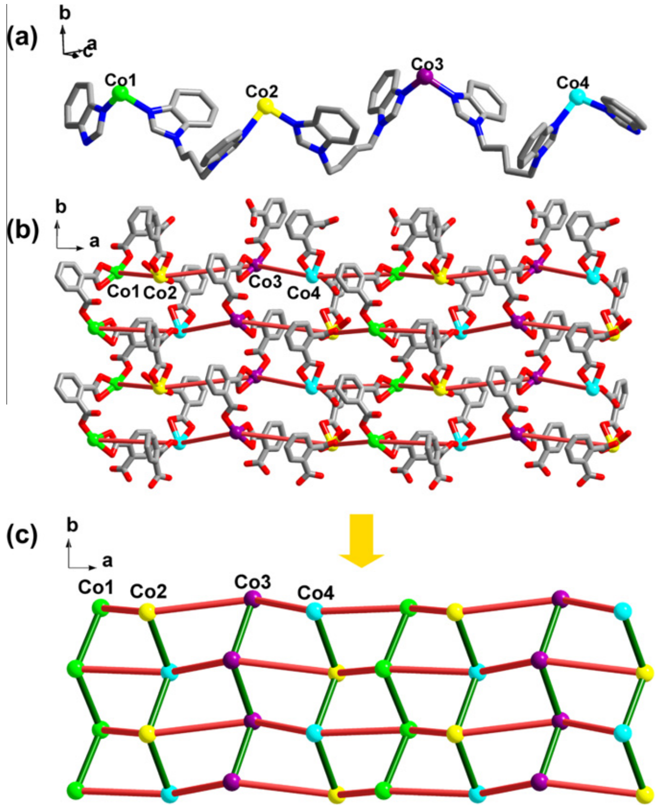

Fig. 2. (a) 1D chain formed by the Co$^{\text{II}}$ ions and bbbm ligands in **1**. (b) 2D layer of **1** constructed from the 1D chains and 1,2-BDC anions along the *ab* plane. (c) 2D 4-connected topological structure of **1**.

unit consists of four Co$^{\text{II}}$ ions, four bbbm ligands, four 1,2-BDC anions, one coordinated water molecule and two interstitial water molecules. The coordination environment of four crystallographically independent Co$^{\text{II}}$ ions is given in Fig. 1. Co1 is five-coordinated by two nitrogen atoms from two bbbm ligands and three oxygen atoms from two 1,2-BDC anions, completing a distorted square pyramid geometry. Co2 is six-coordinated by two nitrogen atoms from two bbbm ligands and four oxygen atoms from two 1,2-BDC anions and one water molecule in a distorted octahedron geometry. The coordination environment of Co3 and Co4 is similar to that of Co1. The Co–N and Co–O bond distances are in the range of 2.023(7)–2.081(7) and 1.936(6)–2.381(6) Å (Table S1), respectively, which are comparable to those of the similar cobalt complexes [30,31].

In **1**, each Co$^{\text{II}}$ ions is bridged by the bbbm ligands to form 1D chains (Fig. 2a), which are further extended by the 1,2-BDC anions into a 2D layer (Fig. 2b). As shown in Fig. 2b, the Co1 and Co3 ions are connected by the 1,2-BDC anions to generate 1D Co1–1,2-BDC and Co3–1,2-BDC chains, respectively, and the 1,2-BDC anions link the Co2 and Co4 ions from adjacent 1D Co-bbbm chains to give the 1D Co2–1,2-BDC–Co4 chains. The Co1–1,2-BDC, Co2–1,2-BDC–Co4 and Co3–1,2-BDC chains are alternately arrayed in the 2D layer. If each Co$^{\text{II}}$ ion is considered as a four-connected node, and the bbbm and 1,2-BDC ligands as linkers, polymer **1** possesses a 2D 4-connected topological structure (Fig. 2c) with a Schfäli symbol of $(4^4{\cdot}6^2)$. In **1**, the 1,2-BDC anion only adopts one type of coordination mode (chelating-monodentate) (Scheme S1), which have been observed in the reported 1,2-BDC metal complexes [32,33].

3.1.2. Crystal structure of **2**

Polymer **2** crystallizes in the monoclinic space group *C*2/*c*. The asymmetric unit consists of one Co$^{\text{II}}$ ion, one bbbm ligand and one 1,4-BDC anion. As depicted in Fig. 3, Co1 is six-coordinated by two nitrogen atoms from two bbbm ligands and four oxygen atoms from two 1,4-BDC anions, furnishing a distorted octahedron geometry. The Co–N bond distances are 2.056(6) (Co1–N1) and 2.069(6) (Co1–N5) Å, and the Co–O bond distances vary in the range of 2.066(5)–2.264(5) Å (Table S1), which are similar to those of **1**.

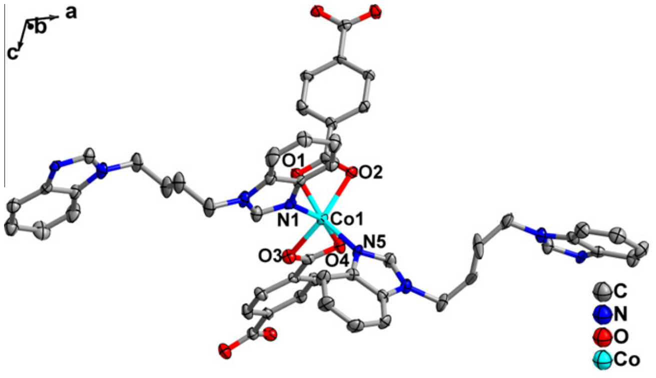

Fig. 3. Coordination environment of the Co$^{\text{II}}$ ion in **2**. All hydrogen atoms are omitted for clarity.

As shown in Fig. 4a, the Co$^{\text{II}}$ ions are connected by the bbbm bridges to form a 1D chain in **2**. The adjacent 1D chains are linked by the 1,4-BDC ligands to give rise to a 2D layer along the *ab* plane (Fig. 4b). It is interesting that, in the 2D layer, there are two kinds of cycles, namely, the small Co$_4$bbbm$_2$BDC$_2$ rings and large Co$_8$bbbm$_6$BDC$_2$ rings. The 2D layers are further connected by the 1,4-BDC ligands to build a 3D framework (Fig. 4c). If we define the Co$^{\text{II}}$ ion as a 4-connected node, and the bbbm and 1,4-BDC ligands as spacers, the 3D framework structure with a Schfäli symbol $(4^2{\cdot}6^3{\cdot}8)$ can be schematically represented by Fig. 5a. By

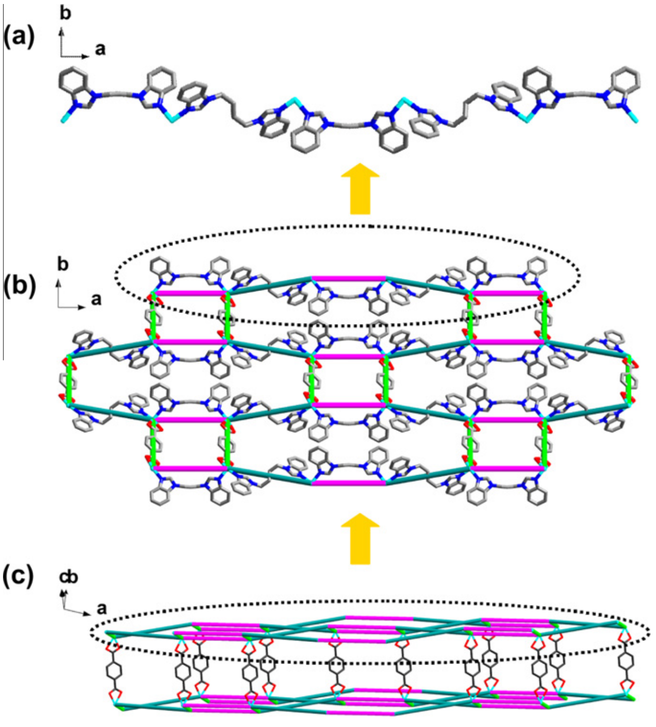

Fig. 4. (a) 1D chain formed by the Co$^{\text{II}}$ ions and bbbm ligands in **2**. (b) 2D layer of **2** constructed from the 1D chains and 1,4-BDC anions. (c) 3D framework built by the 2D layers and 1,4-BDC anions.

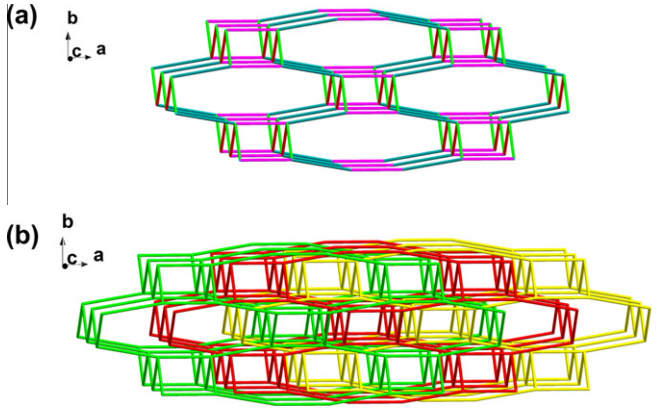

Fig. 5. (a) Single 3D topological framework for **2**. (b) Schematic representation of the 3D 3-fold interpenetrated topological nets for **2**.

careful inspection of the structure for **2**, the single 3D framework incorporating with another two identical networks, gives a 3-fold interpenetrated network (Fig. 5b). To the best of our knowledge, polymer **2** is the rare 3D 3-fold interpenetrated network constructed from the flexible bis(benzimidazole)-based ligand [34,25]. In **2**, the 1,4-BDC anion only adopts one type of chelating-bis(bidentate) coordination mode (Scheme S1), which have been observed in the reported 1,4-BDC metal complexes [35,18].

3.2. Effect of benzenedicarboxylates on the structures of 1 and 2

In this work, bbbm was used as the main ligand, and two kinds of benzenedicarboxylates were used as the auxiliary ligands, aiming at exploring the effect of position of carboxyl groups for benzenedicarboxylates on the assembly of **1** and **2**. According to the above structural description, bbbm uniformly behaves as the bidentate spacers to link the Co^{II} ions in **1** and **2**. When 1,2-BDC anion was used as an ancillary ligand, a 2D 4-connected network of **1** was obtained. In order to investigate the influence of position of carboxyl groups for benzenedicarboxylates on the structures of target compounds, 1,4-BDC was employed as auxiliary ligand in the synthesis of **2**, and a 3D 3-fold interpenetrated framework was constructed. In addition, we have obtained and structurally characterized another bbbm-based cobalt(II) polymer using 1,3-BDC anion as auxiliary ligand, i.e. $[Co(bbbm)(1,3\text{-}BDC)]\cdot H_2O$ (**3**) in our previous work, which exhibits a 2D (4,4) network [36]. Polymers **1** and **3** possess the different 2D network structures, whereas polymer **2** displays a novel 3D 3-fold interpenetrated structure. Obviously, the position of carboxyl groups for benzenedicarboxylates plays an important role in the final structures of **1**, **2** and **3** (Fig. 6).

3.3. Thermogravimetric analyses

To assess the thermal stability of **1** and **2**, thermogravimetric analysis was performed under nitrogen atmosphere in the temperature range of 25–800 °C with a heating rate of 10 °C min^{-1}. As can be seen from the thermal curves (Fig. S1), polymer **1** exhibits three separate steps of weight losses, while polymer **2** features one main step. For **1**, the first weight loss step is observed in the range of 50–130 °C, corresponding to the release of coordinated and interstitial water molecules (found, 2.28 wt.%; calcd, 2.56 wt.%). The second and third successive weight losses from 325 to 750 °C may be attributed to the decomposition of bbbm and 1,2-BDC ligands (found, 83.08 wt.%; calcd., 83.22 wt.%). The crystal networks of **2** are stable up to 430 °C. The successive weight losses in the range of 430–780 °C correspond to the decomposition of bbbm and 1,4-BDC ligands (found, 85.05 wt.%, calcd., 85.40 wt.%). The remaining residues (14.64% for **1**, 14.95% for **2**) correspond to CoO.

3.4. Electrochemical properties

Redox properties of **1** and **2** were investigated in 0.5 M Na_2SO_4 aqueous solution with title complexes bulk-modified CPEs as working electrodes, because polymers **1** and **2** are stable and insoluble in 0.5 M Na_2SO_4 aqueous solution. As shown in Fig. 7 and Fig. S2, the electrochemical behaviors for **1** and **2** are similar except for some slight potential shifts. Thus, only the **1**-CPE is representatively described in detail here. Fig. 7a displays the cyclic voltammograms for **1**-CPE at different scan rates in the potential range of 0 to 900 mV. A pair of reversible redox peaks are observed, which can be attributed to the redox of Co^{III}/Co^{II} [37], and the mean peak potential $E_{1/2} = (E_{pa} + E_{pc})/2$ is +380 mV (100 mV s^{-1}). As seen in Fig. 7a, with the scan rates increasing from 40 to 500 mV s^{-1}, the peak potentials changed gradually: the cathodic peak potentials gradually shift to the negative direction, and the corresponding anodic peak potentials shift to the positive direction. Fig. 7b shows the plots of peak currents versus scan rates, which indicates the redox process of **1**-CPE is surface-controlled.

3.5. Photoluminescent properties

Previous studies have shown that the metal–organic coordination polymers display photoluminescent properties, and may have potential application as fluorescence materials [38].

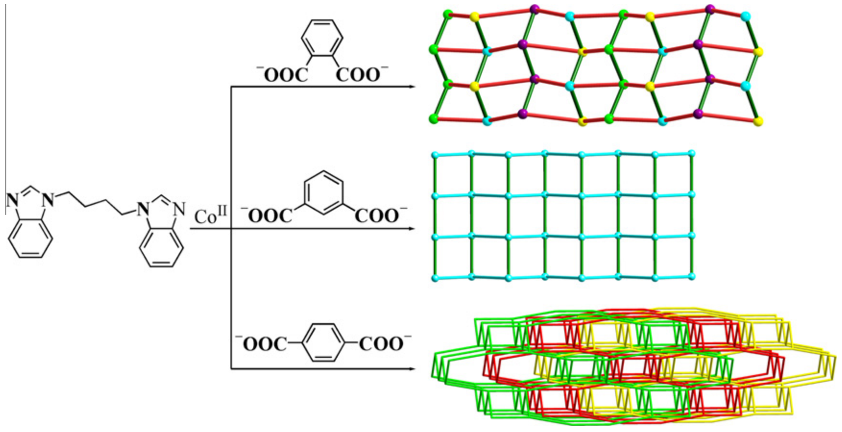

Fig. 6. Effect of carboxyl position of auxiliary benzenedicarboxylates on the structures of **1**–**3**.

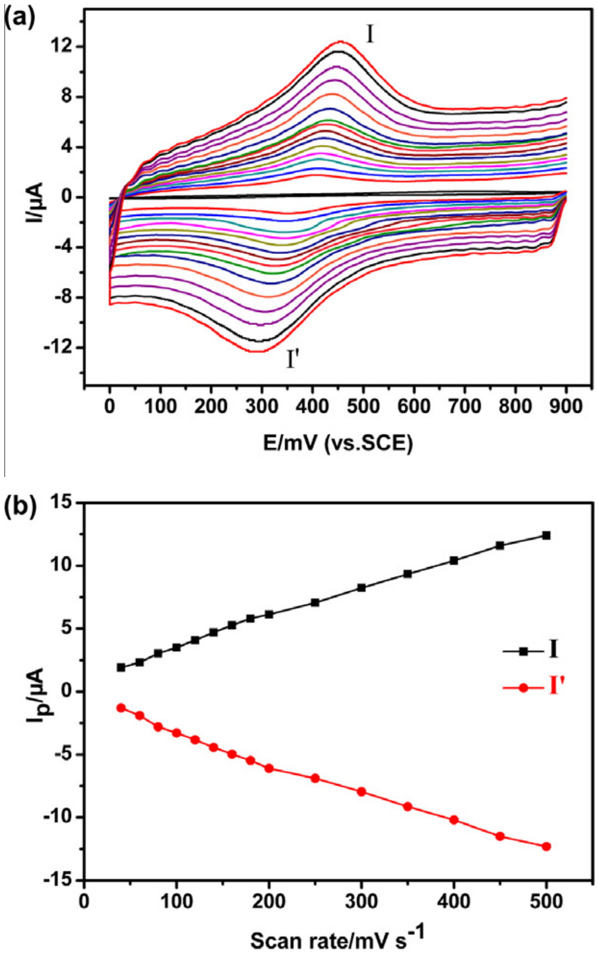

Fig. 7. (a) Cyclic voltammograms of the **1**-CPE in the 0.5 M Na_2SO_4 aqueous solution at different scan rates (from inner to outer: 40, 60, 80, 100, 120, 140, 160, 180, 200, 250, 300, 350, 400, 450, 500 mV s^{-1}). (b) Plots of the anodic and cathodic peak currents against scan rates.

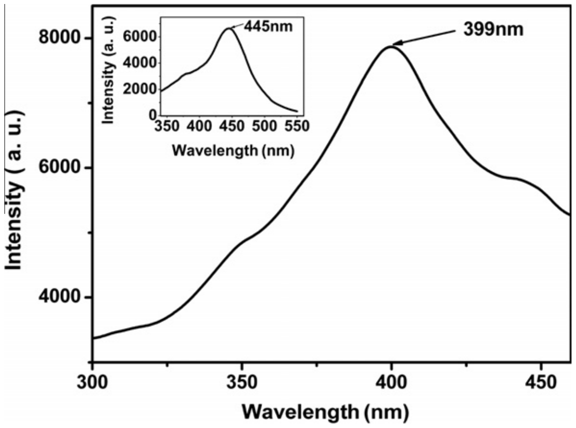

Fig. 8. Fluorescence spectrum for **1** in the solid state at room temperature (inset: fluorescence spectrum of the free bbbm ligand).

Here, the photoluminescent properties of **1** and **2** along with the free bbbm ligand in the solid state at room temperature have been measured. As shown in the inset of Fig. 8, the maximum of emission band is at 445 nm (λ_{ex} = 320 nm) for the free bbbm ligand, which is assigned to the $\pi^* \rightarrow \pi$ electronic transitions of the bbbm. Comparing with the free bbbm ligand, the emission maxima of **1** and **2** uniformly are blue-shifted. They are 399 nm (λ_{ex} = 250 nm) for **1** (Fig. 8), 406 nm (λ_{ex} = 250 nm) for **2** (Fig. S3). The emission bands of **1** and **2** might be attributed to the intraligand charge transfer transitions [39,40].

4. Conclusions

Two new Co^{II} coordination polymers constructed from flexible bbbm and different benzenedicarboxylates have been hydrothermally obtained under similar synthetic conditions. The position of carboxyl groups for auxiliary benzenedicarboxylates shows a great influence on the final structures of **1** and **2**. The polymers **1** and **2** exhibit good electrochemical and photoluminescent properties, demonstrating their potential applications in the electrochemical and luminescent field.

Acknowledgments

This research was financially supported by the National Natural Science Foundation of China (Nos. 21171025 and 21101015), the Program for New Century Excellent Talents in University (NCET-09-0853) and the Natural Science Foundation of Liaoning Province (201102003).

Appendix A. Supplementary material

Supplementary data associated with this article can be found, in the online version, at http://dx.doi.org/10.1016/j.ica.2012.11.024.

References

[1] W.M. Xuan, M.N. Zhang, Y. Liu, Z.J. Chen, Y. Cui, J. Am. Chem. Soc. 134 (2012) 6904.
[2] F. Luo, Z.Z. Yuan, X.F. Feng, S.R. Batten, J.Q. Li, M.B. Luo, S.J. Liu, W.Y. Xu, G.M. Sun, Y.M. Song, H.X. Huang, X.Z. Tian, Cryst. Growth Des. 12 (2012) 3392.
[3] S. Horike, D. Umeyama, M. Inukai, T. Itakura, S. Kitagawa, J. Am. Chem. Soc. 34 (2012) 7612.
[4] G. Givaja, P.A. Ochoa, C.J.G. García, F. Zamora, Chem. Soc. Rev. 41 (2012) 115.
[5] P.O. Adelani, T.E.A. Schmitt, Inorg. Chem. Commun. 49 (2012) 5701.
[6] C.L. Jiao, J. Zhang, S. Wang, X.L. Si, W.S. You, Z.P. Li, Z.G. Wang, H. Yu, Z. Gabelica, H.Y. Zhou, L.X. Sun, F. Xu, Inorg. Chem. Commun. 51 (2012) 5022.
[7] W. Morris, B. Volosskiy, S. Demir, F. Gándara, P.L. McGrier, H. Furukawa, D. Cascio, J.F. Stoddart, O.M. Yaghi, Inorg. Chem. Commun. 51 (2012) 6443.
[8] K.H. He, Y.W. Li, Y.Q. Chen, W.C. Song, X.H. Bu, Cryst. Growth Des. 12 (2012) 2730.
[9] Y. Zhao, C.Q. Jiao, Z.G. Sun, Y.Y. Zhu, K. Chen, C.L. Wang, C. Li, M.J. Zheng, H. Tian, S.H. Sun, W. Chu, Cryst. Growth Des. 12 (2012) 3191.
[10] M. Gustafsson, J. Su, H.J. Yue, Q.X. Yao, X.D. Zou, Cryst. Growth Des. 12 (2012) 3243.
[11] J. Olguín, M. Kalisz, R. Clérac, S. Brooker, Inorg. Chem. Commun. 51 (2012) 5058.
[12] S. Speed, R. Vicente, D. Aravena, E. Ruiz, O. Roubeau, S.J. Teat, M.S.E. Fallah, Inorg. Chem. Commun. 51 (2012) 6842.
[13] F. Yang, B. Li, W. Xu, G.H. Li, Q. Zhou, J. Hua, Z. Shi, S.H. Feng, Inorg. Chem. Commun. 51 (2012) 6813.
[14] S.L. Li, Y.Q. Lan, J.F. Ma, J. Yang, G.H. Wei, L.P. Zhang, Z.M. Su, Cryst. Growth Des. 8 (2008) 675.
[15] X.G. Liu, L.Y. Wang, X. Zhu, B.L. Li, Y. Zhang, Cryst. Growth Des. 9 (2009) 3997.
[16] X.H. Zhou, X.D. Du, G.N. Li, J.L. Zuo, X.Z. You, Cryst. Growth Des. 9 (2009) 4487.
[17] L.L. Li, R.X. Yuan, L.L. Liu, Z.G. Ren, A.X. Zheng, H.J. Cheng, H.X. Li, J.P. Lang, Cryst. Growth Des. 10 (2010) 1929.
[18] Q. Yang, X.F. Zhang, J.P. Zhao, B.W. Hu, X.H. Bu, Cryst. Growth Des. 11 (2011) 2839.
[19] S.Q. Zang, Y.J. Fan, J.B. Li, H.W. Hou, T.C.W. Mak, Cryst. Growth Des. 11 (2011) 3395.
[20] X.L. Wang, Y.Q. Chen, Q. Gao, H.Y. Lin, G.C. Liu, J.X. Zhang, A.X. Tian, Cryst. Growth Des. 10 (2010) 2174.
[21] X.L. Wang, J.X. Zhang, G.C. Liu, H.Y. Lin, Y.Q. Chen, Z.H. Kang, Inorg. Chim. Acta 368 (2011) 207.
[22] X.J. Shi, X. Wang, L.K. Li, H.W. Hou, Y.T. Fan, Cryst. Growth Des. 10 (2010) 2490.
[23] B. Xiao, H.Y. Han, X.R. Meng, Y.L. Song, Y.T. Fan, H.W. Hou, Y. Zhu, Inorg. Chem. Commun. 7 (2004) 378.
[24] C.H. Jiao, C.H. He, J.C. Geng, G.H. Cui, Transition Met. Chem. 37 (2012) 17.
[25] J.H. Qin, L.F. Ma, Y. Hu, L.Y. Wang, CrystEngComm 14 (2012) 2891.

[26] D.E. Wang, K.J. Deng, K.L. Lv, C.G. Wang, L.L. Wen, D.F. Li, CrystEngComm 11 (2009) 1442.

[27] J.B. She, G.F. Zhang, Y.L. Dou, X.Z. Fan, J.Z. Li, Acta Crystallogr., Sect. E 62 (2006) 402.

[28] X.L. Wang, Z.H. Kang, E.B. Wang, C.W. Hu, Mater. Lett. 56 (2002) 393.

[29] G.M. Sheldrick, Acta Crystallogr., Sect. A: Found. Crystallogr. 64 (2008) 112.

[30] C.K. Xia, C.Z. Lu, D.Q. Yuan, Q.Z. Zhang, X.Y. Wu, S.C. Xiang, J.J. Zhang, D.M. Wu, CrystEngComm 8 (2006) 281.

[31] L.L. Wen, F. Wang, J. Feng, K.L. Lv, C.G. Wang, D.F. Li, Cryst. Growth Des. 9 (2009) 3581.

[32] Y.W. Li, H. Ma, Y.Q. Chen, K.H. He, Z.X. Li, X.H. Bu, Cryst. Growth Des. 12 (2012) 189.

[33] C.Y. Xu, Q.Q. Guo, X.J. Wang, H.W. Hou, Y.T. Fan, Cryst. Growth Des. 11 (2011) 1869.

[34] W. Jing, Z.G. Ren, M. Dai, Y. Chen, J.P. Lang, CrystEngComm 13 (2011) 5111.

[35] J. Yang, J.F. Ma, Y.Y. Liu, J.C. Ma, S.R. Batten, Cryst. Growth Des. 9 (2009) 1894.

[36] X.L. Wang, L.L. Hou, J.W. Zhang, J.X. Zhang, G.C. Liu, S. Yang, CrystEngComm 14 (2012) 3936.

[37] T.V. Mitkina, N.F. Zakharchuk, D.Y. Naumov, O.A. Gerasko, D. Fenske, V.P. Fedin, Inorg. Chem. Commun. 47 (2008) 6748.

[38] V.W.W. Yam, K.K.W. Lo, Chem. Soc. Rev. 28 (1999) 323.

[39] H. Jiang, J.F. Ma, W.L. Zhang, Y.Y. Liu, J. Yang, G.J. Ping, Z.M. Su, Eur. J. Inorg. Chem. 5 (2008) 745.

[40] S.W. Jin, D.Q. Wang, W.Z. Chen, Inorg. Chem. Commun. 10 (2007) 685.